scientific reports

OPEN

Quantum correlations and parameter estimation for two superconducting qubits interacting with a quantized field

K. Berrada[1,2]✉, S. Abdel-Khalek[3], M. Algarni[4] & H. Eleuch[5,6,7]

In the present manuscript, we introduce a quantum system of two superconducting qubits (S–Qs) interacting with a quantized field under the influence of the Kerr nonlinear medium and Ising interaction. We formulate the Hamiltonian of the quantum model and determine the density operator of whole quantum system as well as quantum subsystems. We examine the dynamics of the quantumness measures for subsequent times including the S–Qs entanglement, S–Qs-field entanglement and quantum Fisher information in relation to the system parameters. Finally, we display the connection among the measures of quantumness during the time evolution.

Keywords Superconducting qubit, Kerr medium, Ising interaction, Entanglement, Linear entropy, Parameter estimation, Fidelity

Current demonstrations of circuits with up to $\sim 10^2$ physical qubits indicate that S–Qs are a preferred hardware platform for executing quantum computing[1–5]. Large-scale quantum information processing has become more possible with recent advancements in the times of qubit coherence[6,7] and quantum fidelity of one- and two-qubit gates[8,9] in superconducting circuits. S–Qs are controlled using ordinary microwave instruments and are created using regular nanofabrication and microfabrication techniques[10,11]. Achieving a balance between high coherence and straightforward connectivity is the primary challenge in developing a fully functional superconducting quantum computer. Notable advancements in experimentation have been achieved lately in this context[12–16]. Specifically, it has been demonstrated that Xmon qubits exhibit great coherence and outstanding scalability at the same time[17]. In the meanwhile, a gmon coupler allows for the dynamic variation of the coupling between Xmon qubits[18]. Furthermore, a superconducting circuit is thought to be able to be built up to several tens of qubits, to demonstrating its quantum supremacy[19]. S–Qs chains provide a suitable platform for large-scale quantum simulation via these state-of-the-art techniques[20–30].

The non-classical correlations between distinct subsystems are described by quantum entanglement. It has been considered as one of the primary characteristics that set quantum systems apart from classical ones. The generation of quantum entangled states is essential for the accomplishment of quantum protocols with superconducting circuits. These quantum states are important in the domains of quantum cryptography, computation, and fundamental quantum physics[31]. Numerous experiments have accomplished the quantum entanglement of two qubits by linking S–Qs to a shared coupler, by considering a micro-wave resonator[32,33]. Recent investigations have demonstrated the production of multiqubit entangled states with substantial improvements in qubit coherence time[34–37]. Stable entanglement of S–Qs in a microwave resonator has been suggested[38,39], and experimentation has proven this to be possible[40]. Producing steady-state entanglement of S–Qs in separate resonators is important for scalability[41]. In separated resonators, a number of scalable techniques have been proposed in order to stabilize a

[1]College of Science, Department of Physics, Imam Mohammad Ibn Saud Islamic University (IMSIU), Riyadh, Saudi Arabia. [2]The Abdus Salam International Centre for Theoretical Physics, Strada Costiera 11, 34151 Trieste, Italy. [3]College of Science, Department of Mathematics and Statistics, Taif University, P.O. Box 11099, 21944 Taif, Saudi Arabia. [4]College of Science, Department of Mathematical Sciences, Princess Nourah Bint Abdulrahman University, P.O. Box 84428, 11671 Riyadh, Saudi Arabia. [5]Department of Applied Physics and Astronomy, University of Sharjah, 27272 Sharjah, United Arab Emirates. [6]College of Arts and Sciences, Abu Dhabi University, 59911 Abu Dhabi, United Arab Emirates. [7]Institute for Quantum Science and Engineering, Texas A&M University, College Station, TX 77843, USA. ✉email: berradakamal@ymail.com; kaberrada@imamu.edu.sa

two-qubit entangled state[42,43], and this was experimentally accomplished[44]. In this context, the idea is based on the squeeze of the resonator modes after transferring the quantum entanglement to quantum bits. Other suggested strategies consider the resonators microwave fields with a high mean photon number[42,43]. Furthermore, one or two types of the four Bell quantum states can be produced through those schemes.

Recently, the analysis of the accuracy of parameter estimation (P–E)[45] has been the subject of extensive attention by studying the impacts of particle losses and noise sources[46–50]. Based on modifications in the P–E, quantum Fisher information (Q–F–I) is essential for determining the sensitivity of the quantum states. Q–F–I was first utilized by Fisher to examine the P–E[51]. For each given quantum measurement, the Q–F–I is considered for detecting the P–E with maximum information. The assessment for an unknown parameter contributes in the improvement of numerous fields in various quantum technology tasks by ameliorating the approaches utilized to detect the sensitivity of the parameters[52–55]. In this instance, the primary goal of estimation theory is to precisely identify the parameter rate resulting from physical quantum effects. In this regard, the Q–F–I may be used for characterizing the lower bound of the inequality of Cramér–Rao[56]. As a result, the Q–F–I may be thought of as the main issue that has to be resolved. The phenomena of fluctuation and decoherence that arise due to the interactions among the systems and their environment have recently been extensively considered in the literature in relation to the Q–F–I dynamics[57].

Considering the background information mentioned above, we proceed to investigate the physical phenomena related to S–Qs in order to determine the ideal circumstances for using S–Qs in quantum technology operations. We introduce a quantum system of a two S–Qs in the presence of a quantized field under the influence of the Kerr nonlinear medium and Ising coupling. We formulate the Hamiltonian of the quantum model and determine the operator of whole quantum system as well as quantum subsystems by solving the Schrödinger equation. We examine the temporal evolution of the quantumness measures for subsequent times including the S–Qs entanglement, S–Qs field entanglement and Q–F–I in relation to the system parameters. Finally, we exploit the connection among the measures of quantumness.

In the next section, we provide the system dynamics and solution of the Schrödinger equation. "Dynamics of quantumness measures" section presents a review on the quantumness measures and give a discussion on the obtained results. Last section is dedicated to the conclusion.

The quantum model

We propose a realistic quantum system consisting from a two-Cooper pair box that are connected via a Josephson junction with capacitance C_J and energy E_J. A pair of S–Qs in the presence of an electromagnetic field that are in an interaction with a resonator of frequency $\Omega_r = 1/\sqrt{LC}$. The system Hamiltonian can be written as

$$\hat{H} = \frac{\hbar\Omega_r}{2}\left(\hat{o}^{\dagger}\hat{o} + \hat{o}\hat{o}^{\dagger}\right) + \frac{\hbar E_J}{2}\sum_{i=1,2}\hat{\sigma}_z^{i} - \left(\frac{eC_g}{C_g + C_J}\right)\sqrt{\frac{\hbar\omega_r}{LC}}\sum_{j=1,2}\left(\hat{o}^{\dagger} + \hat{o}\right)\hat{\sigma}_x^{j}. \tag{1}$$

$C_g + C_J$ designs the total capacitance with C_g defines the gate capacitance, $\hat{\sigma}_z^{i}$ and $\hat{\sigma}_x^{i}$ represent the Pauli matrices and $o^{\dagger}$ (o) denotes the filed-creation (annihilation) operator. By utilizing the rotating wave approximation[58], the interactive part in the Hamiltonian with the existence of χ is

$$\hat{H}_I = \chi\hat{o}^{\dagger}\hat{o}\left(\hat{o}^{\dagger}\hat{o} - 1\right) + \lambda\sum_{j=1,2}\left(\hat{o}^2\left|+_j\right\rangle\left\langle -_j\right| + \hat{o}^{\dagger 2}\left|-_j\right\rangle\left\langle +_j\right|\right). \tag{2}$$

Here $\lambda = \left(\frac{eC_g}{C_g+C_J}\right)\sqrt{\frac{\hbar\Omega_r}{LC}}$ and that $\left|+_j\right\rangle$ ($\left|-_j\right\rangle$) represents the upper (lower) state of the jth S–Q. The total Hamiltonian is

$$\hat{\mathrm{H}}_T = \frac{\hbar\Omega_r}{2}\left(\hat{o}^{\dagger}\hat{o} + \hat{o}\hat{o}^{\dagger}\right) + \frac{\hbar E_J}{2}\sum_{i=1,2}\hat{\sigma}_z^{i} + \hat{\mathrm{H}}_{\mathrm{I}} + \hat{\mathrm{H}}_N \tag{3}$$

The Hamiltonian $\hat{\mathrm{H}}_N$ introduces the Ising effect as

$$\hat{\mathrm{H}}_N = \hbar\mu_S\left(\hat{\sigma}_{\mathbf{Z}}^{(1)}\hat{\sigma}_{\mathbf{Z}}^{(2)}\right), \tag{4}$$

where the parameter μ_S describes the Ising effect and the z–Pauli operator is represented by $\hat{\sigma}_{\mathbf{Z}}^{(j)} = |+_j\rangle\langle +_j| - |-_j\rangle\langle -_j|$.

We now consider that the field is initially determined by a Glauber coherent state and the S–Qs are in a Bell state. The S–Qs-field initial state is

$$|U(0)\rangle = \frac{1}{\sqrt{2}}[|+_1+_2\rangle + |-_1-_2\rangle] \otimes |\alpha\rangle, \tag{5}$$

where $|\alpha\rangle = \sum_{n=0}^{\infty} A_n\ |n\rangle$ is the coherent state where $A_n = \frac{\alpha^n}{\sqrt{n!}}e^{-\frac{1}{2}\alpha^2}$.

The S–Qs-field state $|U(t)\rangle$ at times $t > 0$ is given by

$$|U(t)\rangle = \sum\nolimits_{n=0}^{\infty}(M_1|n, +_1+_2\rangle + M_2|n+\ell, +_1-_2\rangle + M_3|n+\ell, -_1+_2\rangle + M_4|n+2\ell, -_1-_2\rangle) \tag{6}$$

The coefficients $M_j(n,t), j = 1,2,3,4$ are obtained by solving the Schrödinger equation $i\hbar\partial|U(t)\rangle/\partial t = \widehat{H}\ |\psi(t)\rangle$, where the operator $\widehat{H}$ is defined by equation (4) and we can obtain a system of ordinary differential equations for $M_j(n,t)$

$$\frac{dM_1}{dt} = -i\delta(n)M_1 - i\ \nu_1(n)(\ M_2 +\ M_3)$$

$$\frac{dM_2}{dt} = -i\delta(n+1)M_2 - i\ \nu_1(n)M_1 - i\ \nu_2(n)M_4$$

$$\frac{dM_3}{dt} = -i\delta(n+1)M_3 - i\ \nu_1(n)M_1 - i\ \nu_2(n)M_4$$

$$\frac{dM_4}{dt} = -i\delta(n+2)M_4 - i\ \nu_2(n)(\ M_2 +\ M_3). \tag{7}$$

Here $\delta(n) = \chi n(n-1) + \mu_s$ and $\nu_j(n) = \lambda\sqrt{\frac{(n+2j)!}{(n+2(j-1))!}}$.

The density operator of S–Qs is found by performing the trace over the field basis

$$\widehat{\rho}_{12}(t) = Tr_F|U(t)\rangle\langle U(t)|. \tag{8}$$

This formulation allows us to study the influences of the Ising and Kerr parameters on the measures of quantumness.

Dynamics of quantumness measures

In this present section, we present the dynamics of the quantumness measures for subsequent times including the S–Qs entanglement, S–Qs-field entanglement and Q–F–I under the influences of the kerr nonlinear medium and Ising coupling that are modeled through the manipulation of the parameters χ and μ_S.

In order to study the temporal evolution of the S–Qs entanglement, we consider the concurrence as a measure of entanglement and it is introduced by[59]

$$C_{12}\left(\widehat{\rho}_{12}\right) = max\{0, \Delta_1 - \Delta_2 - \Delta_3 - \Delta_4\}, \tag{9}$$

where Δ_j represents the eigenvalues-square roots of $\widehat{\rho}_{12}\widetilde{\widehat{\rho}_{12}}$ in decreasing order, where $\widetilde{\widehat{\rho}_{12}}$ defines the density operator relating to the Pauli matrix σ_Y and $\widehat{\rho}^*_{12}$ by

$$\widetilde{\widehat{\rho}_{12}} = (\sigma_Y \otimes \sigma_Y)\widehat{\rho}^*_{12}(\sigma_Y \otimes \sigma_Y). \tag{10}$$

Here $\widehat{\rho}^*_{12}$ designs the complex conjugate of $\widehat{\rho}_{12}$.

In Fig. 1, the dynamics concurrence for the S–Qs state is shown in terms of the dimensionless time for different values of χ and μ_S with two-photon transition. Generally, the concurrence C_{12} presents an oscillatory behaviour depending on the parameters χ and μ_S. The entanglement can be generated during the dynamics due to the interaction effect of the S–Qs with the single-mode field. In the absence of the effects of Ising coupling and kerr medium, the measure of entanglement experiences a regular oscillatory structure with sudden birth and sudden death phenomena of quantum entanglement. When the Ising interaction is considered, the amplitudes of the function C_{12} decrease as the time goes on and the oscillations become more faster at large values of the time. We notice that the kerr medium can lead to enhance the oscillations of the function C_{12} and almost preserve the structure of the oscillations as in the standard case ($\chi = \mu_S$=0). The consideration of both effects can have a destructive effect on the S–Qs entanglement during the quantum dynamics. Now, we discuss why the Ising coupling and Kerr nonlinear medium can have a destructive effect on the S–Qs entanglement from the view point of population dynamics. In Fig. 2, the population dynamics for the S–Qs state is shown in terms of the dimensionless time for different values of χ and μ_S. Generally, the population ρ^{11}_{12} presents an oscillatory behaviour depending on the parameters χ and μ_S. It is clear that the presence of two effects leads to inhibit the oscillations' amplitude of the population and therefore suppress the amount of entanglement.

To quantify the S–Qs–field entanglement, we use the linear entropy that is defined by

$$\xi = 1 - \mathrm{Tr}(\widehat{\rho}_{12}). \tag{11}$$

In Fig. 3, we show the dynamics of the S–Qs–field entanglement when the S–Qs is coupled to the radiation field for different values of χ and μ_S with two-photon transition. In general, the linear entropy ε experiences an oscillatory structure that depends on χ and μ_S. We can observe that the temporal variation of the linear entropy is liable to the values of χ and μ_S. Interestingly, the presence of Ising interaction and kerr nonlinear medium lead to enhance the entanglement of the S–Qs–field sate and the oscillations during the dynamics. Moreover, the measure of entanglement tends to reach a stable oscillatory structure at large values of the time. From the obtained result, the manipulation and enhancement the S–Qs–field entanglement can be made through a convenable control on χ and μ_S.

The distribution function, $g_{\widehat{\Theta}}(x)$, can be used for expressing the F–I as[60]

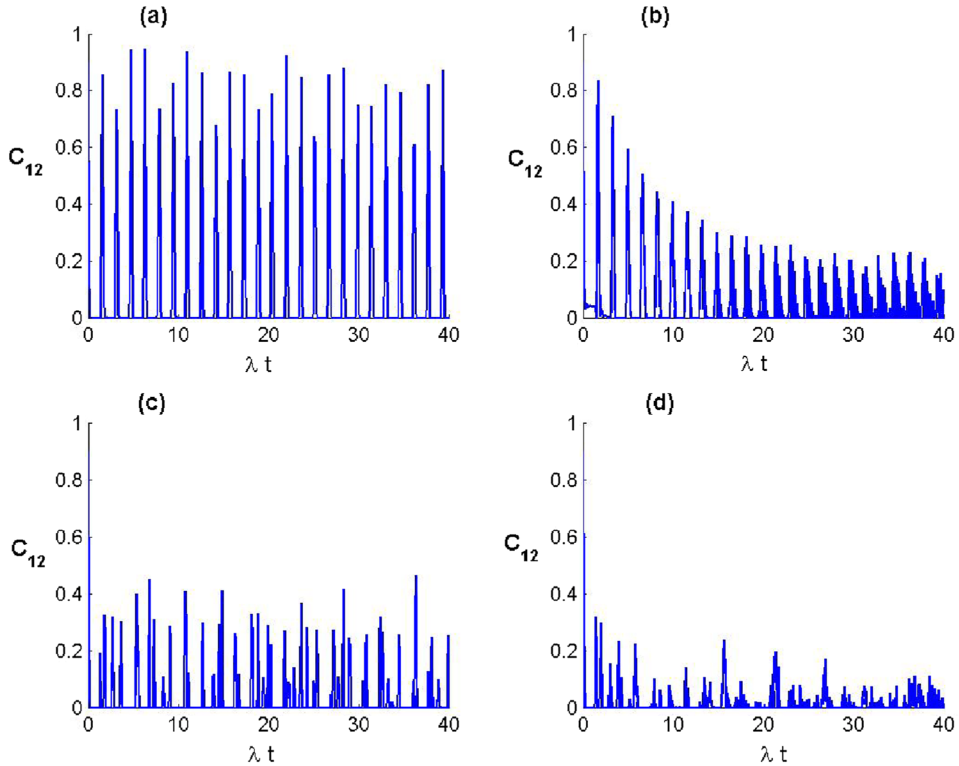

Figure 1. The concurrence C_{12} as a measure of S–Qs entanglement versus λt when the field is initially determined by a coherent state for $\alpha = \sqrt{20}$ for different values of μ_S and χ. (a) is for $(\chi, \mu_S) = (0, 0)$, (b) is for $(\chi, \mu_S) = (0, 15)$, (c) is for $(\chi, \mu_S) = (0.3, 0)$, and (d) is for $(\chi, \mu_S) = (0.3, 15)$.

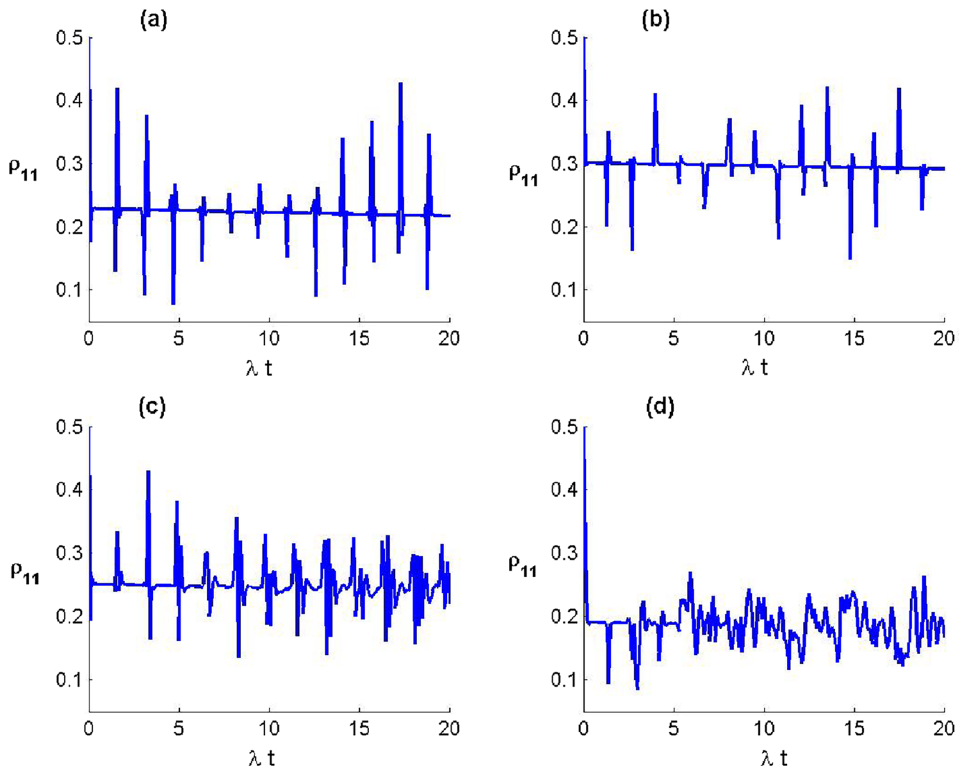

Figure 2. The population ρ_{12}^{11} with similar conditions on the parameters that are defined in the Fig. 1.

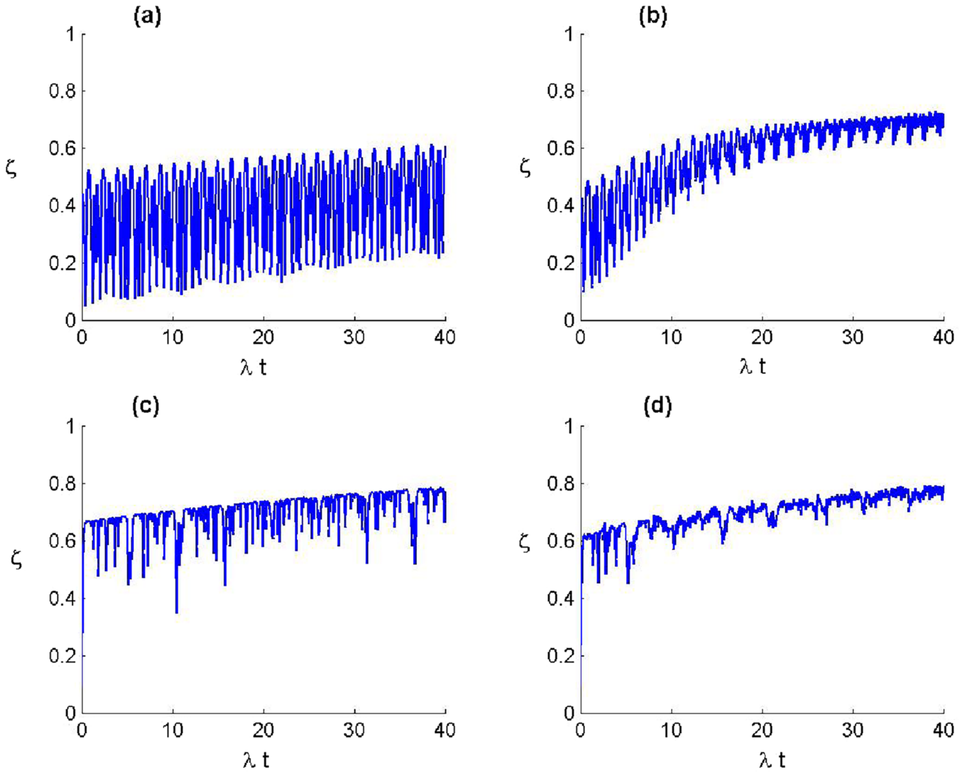

Figure 3. The time evolution of the linear entropy $\boldsymbol{\xi}$ with similar conditions on the parameters that are defined in the Fig. 1.

$$I_{\widehat{\Theta}} = \int \frac{1}{g_{\widehat{\Theta}}(x)} \left(\frac{\partial g_{\widehat{\Theta}}(x)}{\partial \widehat{\Theta}} \right)^2 dx \,, \tag{12}$$

The quantum version of F–I in terms of the estimator $\widehat{\theta}$ can be explored via the symmetric logarithmic derivative $\mathbf{D}(\alpha, \mathbf{t})$ as[61]

$$I_{QF} = \mathbf{Tr}[\widehat{\rho}_{1(2)} \mathbf{D}^2] \tag{13}$$

with

$$2 \frac{\partial \widehat{\rho}_{1(2)}}{\partial \alpha} = \left(\widehat{\rho}_{1(2)} \mathbf{D}(\alpha, \mathbf{t}) + \mathbf{D}(\alpha, \mathbf{t}) \widehat{\rho}_{1(2)} \right), \alpha = \widehat{\Theta}. \tag{14}$$

In Fig. 4, we illustrate the dynamics of Q–F–I for the S–Q state without and with Ising interaction and kerr medium effect. Generally, the measure of Q–F–I is significantly affected by the parameters χ and μ_S. The function I_{QF} exhibits an oscillatory behaviour with amplitudes' values that depend on χ and μ_S. Interestingly, we can observe that the local extrema values of the Q–F–I are extremely dependent on χ and μ_S. Evidently that the maximization, with accuracy of the P–E precision, of the Q–F–I during the dynamics can be realized by a convenable selection of parameter sets of χ and μ_S. Without the effects of Ising interaction and kerr medium, the Q–F–I experiences a regular oscillatory structure. When the Ising interaction is considered, the amplitudes of the function I_{QF} decrease as the time goes. We notice that the kerr nonlinear medium can lead to reduce the oscillations of the function I_{QF}. The consideration of both effects can enhance the oscillations that become more faster for a large time. This result illustrates that the P–E precision in the S–Q state can be controlled through the parameters χ and μ_S.

The fidelity for the S–Qs state is defined by

$$F(t) = \left(Tr \sqrt{\sqrt{\widehat{\rho}_{12}(0)} \widehat{\rho}_{12}(t) \sqrt{\widehat{\rho}_{12}(0)}} \right)^2. \tag{15}$$

In Fig. 5, we show the function F against the dimensionless time λt for different values of χ and μ_S. In general, we mention that the fidelity begins from its maximal value 1 and experiences an oscillatory behaviour. The amount and oscillations amplitude of the function F depend significantly on the values of χ and μ_S. We can observe the value of the fidelity tends to be closer to its maximal value by considering the Ising interaction and kerr medium effect as shown in the figure. In this limit, the function F reaches a stable behaviour and nears to

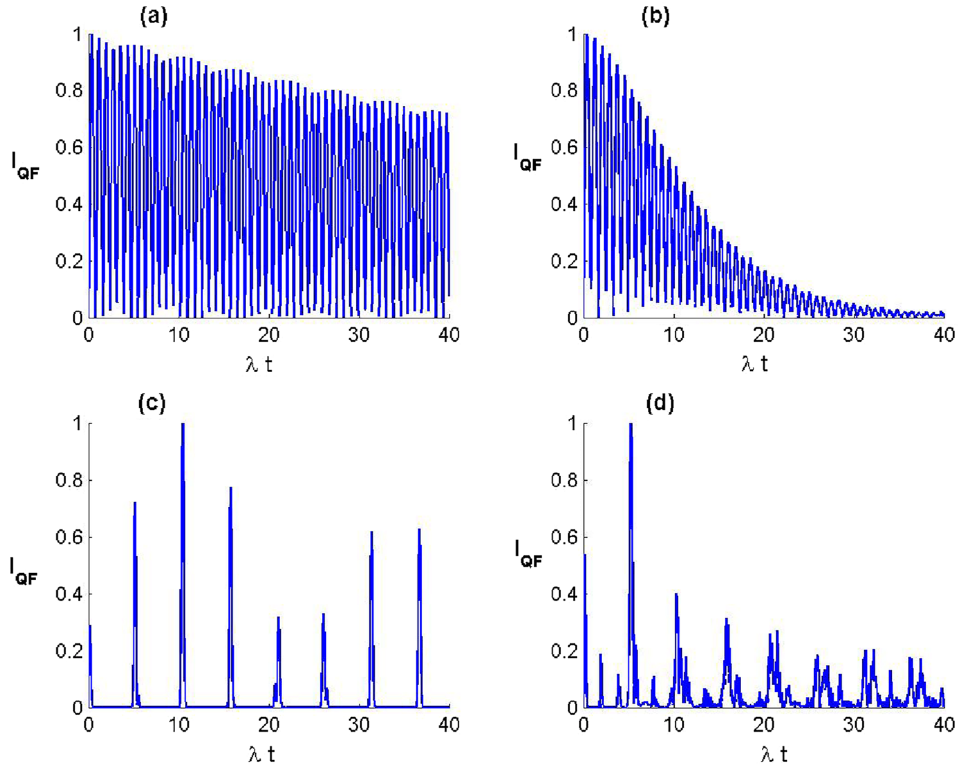

Figure 4. The dynamics of the Q–F–I with similar conditions on the parameters that are defined in the Fig. 1.

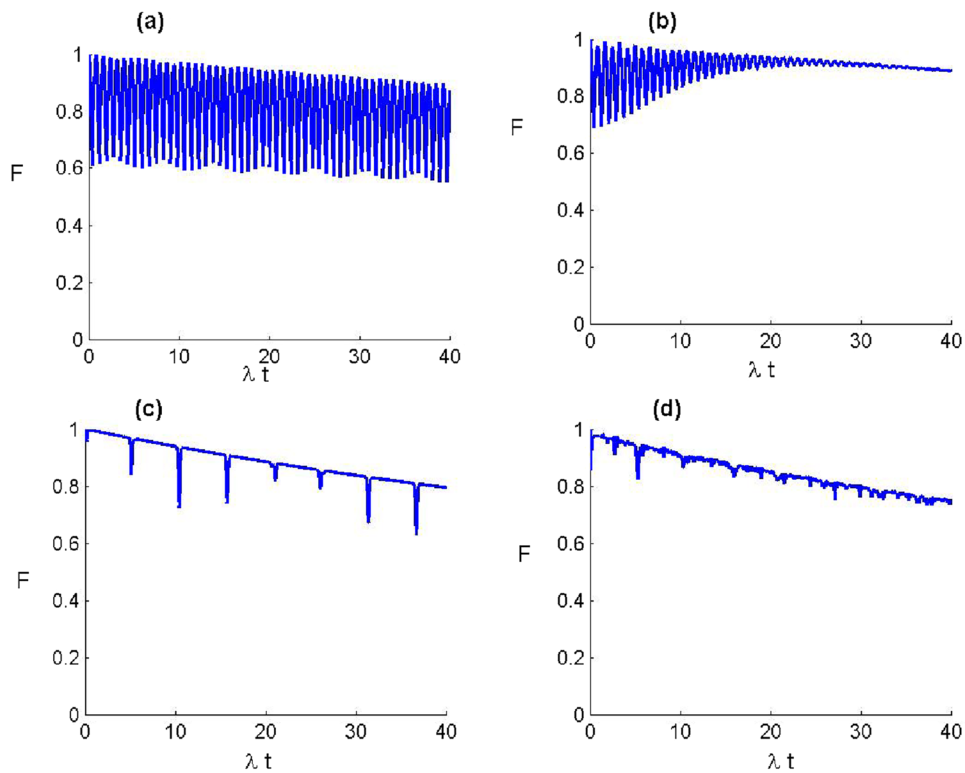

Figure 5. The Fidelity ***F*** with similar conditions on the parameters that are defined in the Fig. 1.

its maximum at large values of the time. This result illustrates how the quantum fidelity can the information or which the S–Qs state to be closed its initial pure state.

Conclusion

In summary, we have explored a quantum system of two S–Qs interacting with a quantized field in the presence of a Kerr nonlinear medium and an Ising coupling. We have formulated the Hamiltonian of the quantum model and evaluated the density operator of whole quantum system as well as quantum subsystems. We have examined the dynamics of the quantumness measures for subsequent times including the S–Qs entanglement, S–Qs field entanglement and Q–F–I in relation to the system parameters. We have discussed how the temporal evolution of the quantifiers can be controlled through a considerable selection of the model physical parameters. Finally, we display the connection among the measures of quantumness during the time evolution. The findings presented here demonstrate the potential use of the system examined in terms of quantum measurements theory in facilitating the execution of experiments under ideal circumstances.

Data availability

The datasets used and/or analyzed during the current study are available from the corresponding author on reasonable request.

Received: 20 November 2023; Accepted: 22 May 2024
Published online: 05 November 2024

References

1. Barends, R. *et al.* Superconducting quantum circuits at the surface code threshold for fault tolerance. *Nature* **508**, 500 (2014).
2. Arute, F. *et al.* Quantum supremacy using a programmable superconducting processor. *Nature* **574**, 505 (2019).
3. Jurcevic, P. *et al.* Demonstration of quantum volume 64 on a superconducting quantum computing system. *Quantum Sci. Technol.* **6**, 025020 (2021).
4. Gong, M. *et al.* Quantum walks on a programmable two-dimensional 62-qubit superconducting processor. *Science* **372**, 948 (2021).
5. Wu, Y. *et al.* Strong quantum computational advantage using a superconducting quantum processor. *Phys. Rev. Lett.* **127**, 180501 (2021).
6. Paik, H. *et al.* Observation of high coherence in Josephson junction qubits measured in a three-dimensional circuit QED architecture. *Phys. Rev. Lett.* **107**, 240501 (2011).
7. Rigetti, C. *et al.* Superconducting qubit in a waveguide cavity with a coherence time approaching 0.1 ms. *Phys. Rev. B* **86**, 100506 (2012).
8. Chow, J. M. *et al.* Complete universal quantum gate set approaching fault-tolerant thresholds with superconducting qubits. *Phys. Rev. Lett.* **109**, 060501 (2012).
9. Magesan, E. *et al.* Efficient measurement of quantum gate error by interleaved randomized benchmarking. *Phys. Rev. Lett.* **109**, 080505 (2012).
10. Oliver, W. D. & Welander, P. B. Materials in superconducting quantum bits. *MRS Bull.* **38**, 816 (2013).
11. Chang, J. B. *et al.* Improved superconducting qubit coherence using titanium nitride. *Appl. Phys. Lett.* **103**, 012602 (2013).
12. Underwood, D. L. *et al.* Imaging photon lattice states by scanning defect microscopy. *Phys. Rev. X* **6**, 021044 (2016).
13. Brecht, T. *et al.* Topology-dependent quantum dynamics and entanglement-dependent topological pumping in superconducting qubit chains. *npj Quantum Inf* **2**, 16002 (2016).
14. Takita, M. *et al.* Demonstration of weight-four parity measurements in the surface code architecture. *Phys. Rev. Lett.* **117**, 210505 (2016).
15. Corcoles, A. D. *et al.* Demonstration of a quantum error detection code using a square lattice of four superconducting qubits. *Nat. Commun.* **6**, 6979 (2015).
16. Chow, J. M. *et al.* Implementing a strand of a scalable fault-tolerant quantum computing fabric. *Nat. Commun.* **5**, 4015 (2014).
17. Barends, R. *et al.* Coherent Josephson qubit suitable for scalable quantum integrated circuits. *Phys. Rev. Lett.* **111**, 080502 (2013).
18. Chen, Y. *et al.* Qubit architecture with high coherence and fast tunable coupling. *Phys. Rev. Lett.* **113**, 220502 (2014).
19. Boixo, S. *et al.* Characterizing quantum supremacy in near-term devices. *Nat. Phys.* **14**, 595 (2018).
20. Fitzpatrick, M., Sundaresan, N. M., Li, A. C. Y., Koch, J. & Houck, A. A. Observation of a dissipative phase transition in a one-dimensional circuit QED lattice. *Phys. Rev. X* **7**, 011016 (2017).
21. Hacohen-Gourgy, S., Ramasesh, V. V., De Grandi, C., Siddiqi, I. & Girvin, S. M. Cooling and autonomous feedback in a bose-hubbard chain with attractive interactions. *Phys. Rev. Lett.* **115**, 240501 (2015).
22. Salathé, Y. *et al.* Digital quantum simulation of spin models with circuit quantum electrodynamics. *Phys. Rev. X* **5**, 021027 (2015).
23. Ferguson, D. G., Houck, A. A. & Koch, J. Symmetries and collective excitations in large superconducting circuits. *Phys. Rev. X* **3**, 011003 (2013).
24. Du, L. H., Zhou, X. X., Han, Y. J., Guo, G. C. & Zhou, Z. W. Strongly coupled Josephson-junction array for simulation of frustrated one-dimensional spin models. *Phys. Rev. A* **86**, 032302 (2012).
25. Chen, G., Chen, Z. D. & Liang, J. Q. Simulation of the superradiant quantum phase transition in the superconducting charge qubits inside a cavity. *Phys. Rev. A* **76**, 055803 (2007).
26. Wang, Y. D., Xue, F., Song, Z. & Sun, C. P. Detection mechanism for quantum phase transition in superconducting qubit array. *Phys. Rev. B* **76**, 174519 (2007).
27. Kapit, E. Universal two-qubit interactions, measurement, and cooling for quantum simulation and computing. *Phys. Rev. A* **87**, 062336 (2013); 92, 012302 (2015).
28. Viehmann, O., von Delft, J. & Marquardt, F. The quantum transverse-field Ising chain in circuit quantum electrodynamics: Effects of disorder on the nonequilibrium dynamics. *Phys. Rev. Lett.* **110**, 030601 (2013).
29. Marcos, D., Rabl, P., Rico, E. & Zoller, P. Superconducting circuits for quantum simulation of dynamical gauge fields. *Phys. Rev. Lett.* **111**, 110504 (2013).
30. Stojanovic, V. M., Vanevic, M., Demler, E. & Tian, L. Transmon-based simulator of nonlocal electron-phonon coupling: A platform for observing sharp small-polaron transitions. *Phys. Rev. B* **89**, 144508 (2014).
31. Horodecki, R., Horodecki, P., Horodecki, M. & Horodecki, K. Quantum entanglement. *Rev. Mod. Phys.* **81**, 865 (2009).
32. Steffen, M. *et al.* Measurement of the entanglement of two superconducting qubits via state tomography. *Science* **313**, 1423 (2006).
33. Ansmann, M. *et al.* Violation of Bell's inequality in Josephson phase qubits. *Nature (London)* **461**, 504 (2009).
34. Neeley, M. *et al.* Generation of three-qubit entangled states using superconducting phase qubits. *Nature (London)* **467**, 570 (2010).

35. Barends, R. *et al.* Superconducting quantum circuits at the surface code threshold for fault tolerance. *Nature (London)* **508**, 500 (2014).
36. Paik, H. *et al.* Experimental demonstration of a resonator-induced phase gate in a multiqubit circuit-QED system. *Phys. Rev. Lett.* **117**, 250502 (2016).
37. Song, C. *et al.* 10-qubit entanglement and parallel logic operations with a superconducting circuit. *Phys. Rev. Lett.* **119**, 180511 (2017).
38. Leghtas, Z. *et al.* Stabilizing a Bell state of two superconducting qubits by dissipation engineering. *Phys. Rev. A* **88**, 023849 (2013).
39. Reiter, F., Tornberg, L., Johansson, G. & Sørensen, A. S. Steady-state entanglement of two superconducting qubits engineered by dissipation. *Phys. Rev. A* **88**, 032317 (2013).
40. Shankar, S. *et al.* Autonomously stabilized entanglement between two superconducting quantum bits. *Nature (London)* **504**, 419 (2013).
41. Aron, C., Kulkarni, M. & Türeci, H. E. Photon-mediated interactions: A scalable tool to create and sustain entangled states of N atoms. *Phys. Rev. X* **6**, 011032 (2016).
42. Hein, S. M., Aron, C. & Türeci, H. E. Purification and switching protocols for dissipatively stabilized entangled qubit states. *Phys. Rev. A* **93**, 062331 (2016).
43. Aron, C., Kulkarni, M. & Türeci, H. E. Steady-state entanglement of spatially separated qubits via quantum bath engineering. *Phys. Rev. A* **90**, 062305 (2014).
44. Kimchi-Schwartz, M. E. *et al.* Stabilizing entanglement via symmetry-selective bath engineering in superconducting qubits. *Phys. Rev. Lett.* **116**, 240503 (2016).
45. Giovannetti, V., Lloyd, S. & Maccone, L. Advances in quantum metrology. *Nat. Photonics* **5**, 222 (2011).
46. Modi, K., Cable, H., Williamson, M. & Vedral, V. Quantum correlations in mixed-state metrology. *Phys. Rev. X* **1**, 021022 (2011).
47. Pires, D. P., Silva, I. A., deAzevedo, E. R., Soares-Pinto, D. O. & Filgueiras, J. G. Coherence orders, decoherence, and quantum metrology. *Phys. Rev. A* **98**, 032101 (2018).
48. Fiderer, L. J. & Braun, D. Quantum metrology with quantum-chaotic sensor. *Nat. Commun.* **9**, 1351 (2018).
49. Joo, J., Munro, W. J. & Spiller, T. P. Quantum metrology with entangled coherent states. *Phys. Rev. Lett.* **107**, 083601 (2011).
50. Berrada, K., Abdel Khalek, S. & Raymond Ooi, C. H. Quantum metrology with entangled spin-coherent states of two modes. *Phys. Rev. A* **86**, 033823 (2012).
51. Fisher, R. A. *Proc. Cambridge Phil. Soc.* **22**, 700 (1929) reprinted in Collected Papers of R. A. Fisher, edited by J. H. Bennett (Univ. of Adelaide Press, South Australia, 1972), pp. 15–40.
52. Giovannetti, V., Lloyd, S. & Maccone, L. Quantum-enhanced measurements: beating the standard quantum limit. *Science* **306**, 1330 (2004).
53. Dowling, J. Quantum optical metrology—The lowdown on high-N00N states. *Contemp. Phys.* **49**, 125 (2008).
54. Jones, J. A. *et al.* Magnetic field sensing beyond the standard quantum limit using 10-spin NOON states. *Science* **324**, 1166 (2009).
55. Simmons, S., Jones, J. A., Karlen, S. D., Ardavan, A. & Morton, J. J. L. Magnetic field sensors using 13-spin cat states. *Phys. Rev. A* **82**, 022330 (2010).
56. Cramer, H. *Mathematical Methods of Statistics* (Princeton University Press, 1946).
57. Chin, A. W., Huelga, S. F. & Plenio, M. B. Entanglement of formation and concurrence. *Phys. Rev. Lett.* **109**, 233601 (2012).
58. Allen, L. & Eberly, J. H. *Optical Resonance and Two-Level Atoms* (Wiley, 1975).
59. Wootters, W. K. Entanglement of formation and concurrence. *Quantum. Inform. Comput.* **1**, 27 (2001).
60. Fisher, R. A. *Proc. Cambridge Phil. Soc*. 1929, 22, 700 reprinted in Collected Papers of R. A. Fisher, edited by J. H. Bennett (Univ. of Adelaide Press, South Australia), 15–40 (1972).
61. Barndorff-Nielsen, O. E., Gill, R. D. & Jupp, P. E. On quantum statistical inference. *J. R. Stat. Soc. B* **65**, 775 (2003).

Acknowledgements

This work was supported by Princess Nourah bint Abdulrahman University Researchers Supporting Project No. PNURSP2024R225, Princess Nourah bint Abdulrahman University, Riyadh, Saudi Arabia.

Author contributions

K.B. and S.A.-K. wrote the manuscript. M.A. and H.E. reviewed the manuscript.

Competing interests

The authors declare no competing interests.

Additional information

Correspondence and requests for materials should be addressed to K.B.

Reprints and permissions information is available at www.nature.com/reprints.

Publisher's note Springer Nature remains neutral with regard to jurisdictional claims in published maps and institutional affiliations.